Heliocentric Zoning of the Asteroid Belt by Aluminum-26 Heating

Robert E. Grimm and Harry Y. McSween, Jr.

The dependence of asteroid spectral class (and inferred composition and thermal history) on heliocentric radius has been held to be the result of heating by a solar energy source, most likely electrical induction, during the formation of the planetary system. Such variations in thermal history can be more simply explained by the presence of different amounts of the radionuclide aluminum-26, whose decay products are observed in meteorites, in planetesimals. These differences occurred naturally as a function of the increasing amount of time required to accrete objects farther from the sun, during which aluminum-26 decayed from its initial concentration in the solar nebula. Both theory and isotopic evidence suggest that increases in accretion time across the asteroid belt are of order several half-lives of aluminum-26, which is sufficient to produce the inferred differences in thermal history.

Variations in petrology among meteorites point to a strong heating event early in solar system history, but the heat source has remained unidentified (*1*, *2*). The high-energy, short-lived radionuclide ^{26}Al (half-life 0.72 million years) has been considered the most likely source since the discovery of its decay product, excess ^{26}Mg, in Allende calcium-aluminum inclusions (CAIs) (*3*). Furthermore, observation of relic ^{26}Mg in an achondritic clast and in feldspars within ordinary chondrites (*4*, *5*) provided strong evidence for radioactive ^{26}Al in meteorite parent bodies and not just in refractory nebular condensates. The inferred amount of ^{26}Al is consistent with constraints on the thermal evolution of both ordinary (6) and carbonaceous (*7*, *8*) chondrite parent objects up to a few hundred kilometers in diameter. Also present in meteorite parent bodies was ^{60}Fe (9), although its thermal effect was probably much smaller than that of ^{26}Al (*10*).

Information in meteorites can constrain the early thermal evolution of asteroids from the same location as the meteorite's parent body, presumably within the asteroid belt (*11*, *12*), provided that a link can be established between asteroid spectrophotometric signature and meteorite class (*13*). Asteroid compositions are heliocentrically distributed (*14*): objects thought to have experienced high metamorphic or even melting temperatures are located closer to the sun, whereas apparently unaltered or mildly heated asteroids are located farther away (*15*). There is some uncertainty attributable to orbital reshuffling of asteroids, but a gross zonal structure within the belt is clearly preserved. The discovery of the heliocentric structure of the asteroid belt suggested that the sun was the energy source for heating and led some workers to reject radionuclide heat sources (*16*). The comparatively long heating intervals and slow cooling rates of most meteorites rule out the possibility that small objects could be directly heated by excess solar luminosity (*1*); instead, it has been argued that large planetesimals were heated by dc electrical induction, a process in which currents are driven through an object as a result of its movement through enhanced magnetic fields and charged solar wind, which are presumably associated with T Tauri behavior of the early sun (*17*–*19*).

In this report, we quantitatively demonstrate that heliocentric zoning in the asteroid belt could equally well be the result of radionuclide heating. Evidence from other long-lived radionuclides suggests that the initial distribution of ^{26}Al in the nebula was uniform (*20*) and that disturbed Al-Mg systematics in CAIs results from secondary processing (*21*). Variable ^{26}Al heating would have occurred if the initial amount of the radionuclide incorporated into planetesimals was controlled by accretion time, which in turn varies with the semimajor axis of the body's orbit. In the simplest analytical theory of planetary accretion by continuous sweeping-up of matter in a gas-free environment (*22*), the accretion rate dr/dt varies as

$$\frac{dr}{dt} \propto \frac{v_c\,(1 + 2\theta)M_p}{a^2\Delta a} \qquad (1)$$

where M_p is the mass of all matter in an accretion zone of width Δa, a is the semimajor axis, the circular orbital velocity $v_c = \sqrt{GM_s/a}$ where G is the gravitational constant and M_s is the mass of the sun, and $1 + 2\theta$ is a factor accounting for gravitational enhancement of the growing object's geometric cross section. Substituting for v_c, Eq. 1 can be integrated to give the time τ required for a planetesimal to grow to a specified radius:

$$\tau \propto a^n \qquad (2)$$

where n = 1.5 to 3, depending on the assumptions about variations in the surface density of the planetesimal swarm (*23*). Numerical simulations of planetesimal accretion at fixed semimajor axis (*24*, *25*) demonstrate that variations in accretion time among small planetesimals can be strongly nonlinear, leading to runaways, depending on the initial conditions and model assumptions. The general relationship with the semimajor axis remains valid because it depends only on the initial orbital properties and the distribution of the planetesimal swarm.

It could be argued that ^{26}Al decay is so rapid that the processes of planetesimal formation (and not accretion of larger parent asteroids, as given in Eq. 1) should be considered. The collapse of patches of the solar nebula into ~10-km-diameter planetesimals is thought to occur when gravitational forces overcome pressure and differential rotation (*26*, *27*). The lowest nebula surface density for which this can be achieved is proportional to the orbital angular velocity, from which it can be shown that the time scale for gravitational collapse varies as $a^{3/2}$. Such radial variations in planetesimal formation time will have the same qualitative effect on the initial amount of incorporated ^{26}Al as gradients in accretion time.

In order to demonstrate the basic dependence of thermal evolution on semimajor axis, we parameterized accretion time across the asteroid belt with Eq. 2 and calculated the subsequent thermal history. Objects at a specified semimajor axis were assumed to have the same accretion time, regardless of size. Several lines of reasoning constrain the accretion time τ_0 at semimajor axis a_0. Numerical simulations indicate that 1000-km-diameter objects can accumulate at 2.5 astronomical units (AU) within 0.1 to 1 million years (*28*), although most of the accreting mass is still in smaller bodies. Earlier work (*24*) suggested that runaways could be even more rapid. Time constraints imposed by radionuclide chronometers, especially ^{26}Al, are also useful. During the time between the condensation of refractory inclusions in chondritic meteorites and their incorporation into parent objects (that is, compaction of meteorite matrix material), the ^{26}Al to ^{27}Al ratio fell from 6×10^{-5} (3) to 8×10^{-6} (4), which implies that τ_0 = 2.1 million years at $a_0 \sim$ 2 AU. Thermal models for chondrites (6–8) support these conclusions, and the inferred ^{26}Al to ^{27}Al ratio at the time of parent-body accumulation is of the order several parts per million. The longer accretion times, compared with predictions based solely on gravitational sweep-up, presumably arise from the time necessary for full condensation of the nebula and its coagulation or gravitational collapse into

R. E. Grimm, Department of Geology, Arizona State University, Tempe, AZ 85287.
H. Y. McSween, Jr., Department of Geological Sciences, University of Tennessee, Knoxville, TN 37996.

early planetesimals (*29, 30*). We set the initial ratio of ^{26}Al to ^{27}Al at 6×10^{-5} (*3*) and treated n and τ_0 at $a_0 = 3$ AU as adjustable parameters with trial values based on the discussion above.

The principal observational constraints to be met by the model are the inferred heliocentric distances at which chondritic silicates and water ice within asteroids melt, transitions which are assumed to occur at temperatures of 1100° and 0°C, respectively. The position of the silicate-melting isotherm is uncertain because of the controversy concerning the nature of S-asteroids and the origin of ordinary chondrites (*28*). One recent summary (*15*) considers S-types to be differentiated and divides the asteroids into igneous, metamorphic, and primitive types with boundaries at about 2.7 and 3.4 AU. The boundary between igneous and metamorphic classes should therefore correspond roughly to the 1100°C isotherm. Ordinary chondrites are thought to originate closer to the sun than this boundary but from smaller objects that experienced greater heat loss and were unmelted. However, this scheme may not be consistent with thermal models (6) that call for diameters of 100 to 200 km for ordinary chondrite parent bodies and heliocentric distances near 2.0 AU.

Several lines of evidence indicate that ice was formerly present in meteorite parent bodies and exists today in the asteroid belt: spectral signatures of H_2O frost on C-asteroids (*31*), textures of carbonaceous chondrites (*32*), and kinetic calculations demonstrating the difficulty of condensing hydrated silicates directly from the nebula (*33*). The incorporation of ice into planetesimals can strongly affect thermal history (*7*) because ice provides a thermal buffer that substitutes low-temperature aqueous alteration (as in carbonaceous chondrites) for high-temperature metamorphic recrystallization (as in ordinary and enstatitic chondrites). Evidence of hydrated silicates in some low-albedo asteroids (*16, 31*) is now taken to support the idea that aqueous alteration occurred when melted ice reacted with anhydrous silicates. Such asteroids are generally dominant around 3 AU, but objects farther out show spectral signatures of decreased amounts of hydrated silicates, which suggests that liquid water was not present there. The isotherm for ice melting is the basis for the division between metamorphic and primitive asteroid types (*15*) at 3.4 AU.

The distribution of ice in the asteroid belt before the heating event is uncertain. Therefore, we have performed two sets of thermal calculations. In the first (the anhydrous model), the thermal effects of ice were neglected: all model objects were assumed to be 90% rock and 10% voids. In the second set (the hydrous model), we explicitly introduced ice beyond 2.7 AU. This distance corresponds to the igneous-metamorphic division in asteroids (*15*), which in turn is based largely on the S (anhydrous) to C (hydrous) transition in asteroid types. Model objects beyond here had compositions of 60% rock, 30% ice, and 10% voids by volume. These values are consistent with the density of the C-asteroid Ceres, 2.3 ± 1.1 Mg/m^3 (*34*), assuming an intrinsic density of 3.3 Mg/m^3 for the rocky portion.

The model (*7*) included temperature-dependent thermal properties of ice and rock (CM chondrite analog) and thermodynamic effects of phase transitions. Mechanisms of H_2O transport (hydrothermal convection, gas diffusion, and venting attributable to hydraulic or gas fracturing) and long-lived radionuclide heating were neglected.

The positions of the silicate- and ice-melting isotherms for the anhydrous model (Fig. 1A) with $\tau_0 = 3.5$ million years and for the hydrous model (Fig. 1B) with $\tau_0 = 3.0$ million years agree with observations at large diameters. A shorter accretion time is required for the hydrous model because a larger amount of ^{26}Al is necessary to achieve the specified threshold temperatures when ice is present. Both of these times are upper bounds because objects will radioactively heat during formation and reach limiting temperatures more rapidly than in our model, in which full-grown objects are initially cold. This limit is consistent with expectations from dynamic models with somewhat shorter accretion times (*24, 25, 28*).

In both the anhydrous and hydrous models, the best fit was achieved with $n = 3$ in Eq. 2, although $n = 2.5$ gave comparable results if τ_0 was increased slightly. The large value of n is required to accommodate the strong variation in temperature over less than 1 AU and is in agreement with suggestions that the surface density of the planetesimal swarm varied as a^{-1} to $a^{-3/2}$ (*28, 35*). Such values of n lead to variations in accretion time of several half-lives of ^{26}Al across the asteroid belt (Fig. 1, top).

These calculations demonstrate that heliocentric zoning of the asteroid belt can be achieved by ^{26}Al heating with reasonable assumptions about the variation of accretion time with semimajor axis. Although

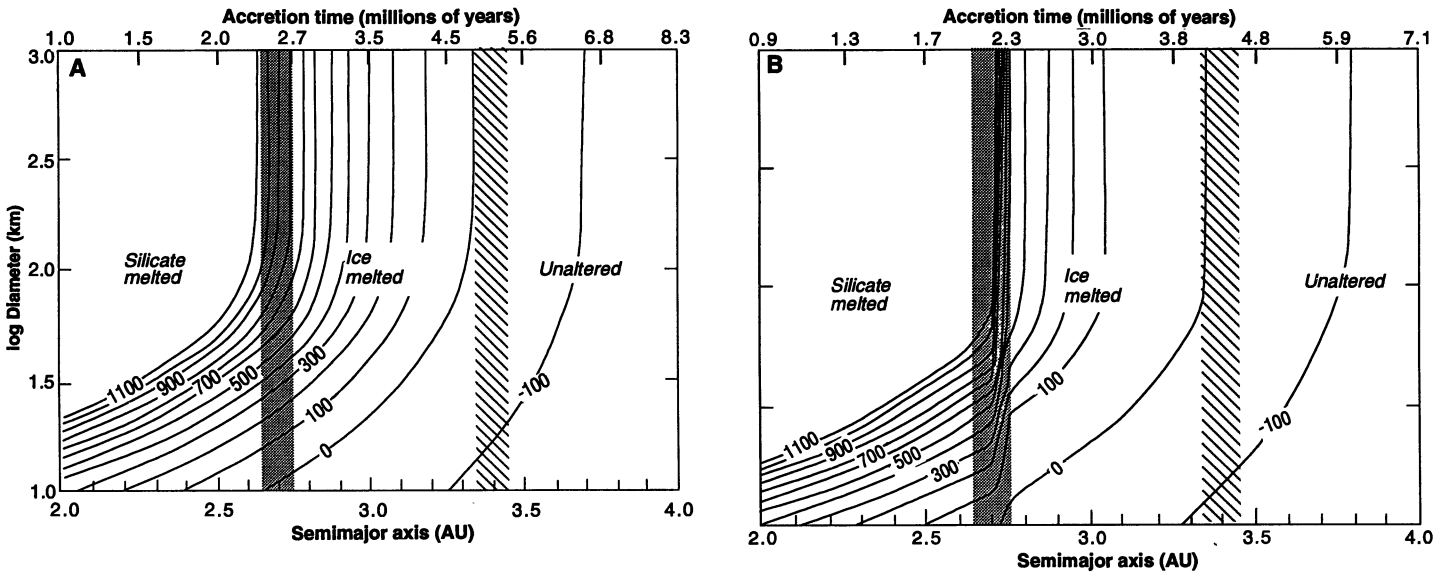

Fig. 1. Contours of peak temperatures (°C) in model objects as functions of size and semimajor axis for (**A**) anhydrous model and (**B**) hydrous model. Dependence of accretion time on semimajor axis described in text. Shaded bands mark major divisions of the asteroid belt based on spectrophotometric data (*15*). Both models can approximately reproduce range of inferred peak temperatures experienced by asteroids.

heating by solar electromagnetic induction has gained favor with the recognition of a sun-centered heating pattern in the asteroid belt, that model is highly simplified (for example, it assumes a time-independent magnetic field, axisymmetry of electric potential within the target object, and the validity of a first-term truncation of the Legendre series solution) and contains considerable uncertainties in parameter choices (early solar electric and magnetic flux, strong temperature, and compositional dependence of electrical conductivity) (*17*). We cannot reject this hypothesis with present data, but we favor ^{26}Al heating because it can explain the observed data with fewer assumptions and because ^{26}Al is known to have been present in significant quantities in newly accreted meteorite parent bodies (*4*).

REFERENCES AND NOTES

1. C. P. Sonett and R. T. Reynolds, in *Asteroids*, T. Gehrels, Ed. (Univ. of Arizona Press, Tucson, 1979), pp. 822–848.
2. J. A. Wood and P. Pellas, in *The Sun in Time*, C. P. Sonett, M. S. Giampapa, M. S. Matthews, Eds. (Univ. of Arizona Press, Tucson, 1992), pp. 740–760.
3. T. Lee, D. A. Papanastassiou, G. J. Wasserburg, *Geophys. Res. Lett.* **3**, 109 (1976).
4. I. D. Hutcheon, R. Hutchison, G. J. Wasserburg, *Nature* **337**, 238 (1989).
5. E. Zinner and C. Gopel, *Meteoritics* **27**, 311 (1992).
6. M. Miyamoto, N. Fujii, H. Takeda, *Proc. Lunar Planet. Sci. Conf.* **12B**, 1145 (1981).
7. R. E. Grimm and H. Y. McSween, Jr., *Icarus* **82**, 244 (1989).
8. M. Miyamoto, *Meteoritics* **26**, 111 (1991).
9. A. Shukolyukov and G. W. Lugmair, *Lunar Planet. Sci.* **XXIII**, 1295 (1992).
10. The initial ^{26}Al to ^{27}Al ratio in CAIs (*3*) was reported to be 6×10^{-5}, whereas the initial ^{60}Fe to ^{56}Fe ratio in CAIs (*9*) was inferred to be 1.6×10^{-6}. The decay energies are both about 3 MeV per atom, and the half-lives are 0.72 million years for ^{26}Al and 1.5 million years for ^{60}Fe. Assuming these proportions were incorporated into carbonaceous chondrites with 210 mg of bulk Fe and 12 mg of Al per gram of chondrite, the initial heat productions would be 2.6×10^{-8} and 2.5×10^{-7} W/kg, respectively, a tenfold difference. By the time the slower decay of ^{60}Fe allows it to dominate (~5 million years), heat production from both isotopes is inconsequential, $\sim 10^{-9}$ W/kg.
11. R. Greenberg and C. R. Chapman, *Icarus* **55**, 455 (1983).
12. J. Wisdom, *Nature* **315**, 731 (1985).
13. M. J. Gaffey and T. B. McCord, *Space Sci. Rev.* **21**, 555 (1978).
14. J. Gradie and E. Tedesco, *Nature* **216**, 1405 (1982).
15. J. F. Bell, D. R. Davis, W. K. Hartmann, M. J. Gaffey, in *Asteroids II*, R. P. Binzel, T. Gehrels, M. S. Matthews, Eds. (Univ. of Arizona Press, Tucson, 1989), pp. 921–945.
16. T. D. Jones, L. A. Lebofsky, J. S. Lewis, M. S. Marley, *Icarus* **88**, 172 (1990).
17. C. P. Sonett, D. S. Colburn, K. Schwartz, K. Keil, *Astrophys. Space Sci.* **7**, 446 (1970).
18. F. Herbert and C. P. Sonett, *Icarus* **40**, 484 (1979).
19. F. Herbert, *ibid.* **78**, 402 (1989).
20. F. A. Podosek *et al.*, *Geochim. Cosmochim. Acta* **55**, 1083 (1991).
21. G. J. MacPherson, A. M. Davis, E. K. Zinner, *Meteoritics* **27**, 253 (1992).
22. G. W. Wetherill, *Annu. Rev. Astron. Astrophys.* **18**, 77 (1980).
23. The surface density is given by $\sigma = M_c/4\pi a\,\Delta a$. For constant σ, $n = 3/2$; for $\sigma \sim a^{-1}$ (*28*), $n = 5/2$; and for $\sigma \sim a^{-3/2}$ (*35*), $n = 3$. The Titius-Bode geometrical progression of semimajor axes implies $\Delta a \sim a$, which also gives $n = 5/2$.
24. R. Greenberg, J. F. Wacker, W. K. Hartmann, C. R. Chapman, *Icarus* **35**, 1 (1978).
25. G. W. Wetherill and G. R. Stewart, *ibid.* **77**, 330 (1989).
26. P. Goldreich and W. R. Ward, *Astrophys. J.* **183**, 1051 (1973).
27. D. J. Stevenson, A. W. Harris, J. I. Lunine, in *Satellites*, J. Burns and M. S. Matthews, Eds. (Univ. of Arizona Press, Tucson, 1986), pp. 39–88.
28. G. W. Wetherill and C. R. Chapman, in *Meteorites and the Early Solar System*, J. F. Kerridge and M. S. Matthews, Eds. (Univ. of Arizona Press, Tucson, 1988), pp. 35–67.
29. S. J. Weidenschilling, *ibid.*, pp. 348–371.
30. J. A. Wood and G. E. Morfill, *ibid.*, pp. 329–347.
31. L. A. Lebofsky, M. A. Feierberg, A. T. Tokunaga, H. P. Larson, J. R. Johnson, *Icarus* **48**, 453 (1981).
32. T. E. Bunch and S. Chang, *Geochim. Cosmochim. Acta* **44**, 1543 (1980).
33. R. G. Prinn and B. Fegley, Jr., *Annu. Rev. Earth Planet. Sci.* **15**, 171 (1987).
34. J. Schubart and D. L. Matson, in (*1*), pp. 84–97.
35. S. J. Weidenschilling, *Astrophys. Space Sci.* **51**, 153 (1977).

3 September 1992; accepted 1 December 1992

Isotope Effect and Superconductivity in Metal-Doped C_{60}

Chia-Chun Chen and Charles M. Lieber*

The mechanism of superconductivity in alkali metal–doped fullerenes remains a fascinating and controversial issue. One powerful probe of this mechanism involves the determination of the shift in transition temperature (δT_c) upon isotopic substitution. A series of isotopically substituted Rb_3C_{60} superconductors, where C_{60} corresponds to $^{13}C_{60}$, $(^{13}C_{60})_{0.5}(^{12}C_{60})_{0.5}$, or $(^{13}C_{0.55}{}^{12}C_{0.45})_{60}$, was investigated. The δT_c determined for $Rb_3{}^{13}C_{60}$, 0.7 ± 0.1 K, provides an unambiguous value for the isotope shift in fully substituted fullerene superconductors. The δT_c determined for $Rb_3(^{13}C_{0.55}{}^{12}C_{0.45})_{60}$, 0.5 K, is also consistent with simple mass scaling of the $Rb_3{}^{13}C_{60}$ result. However, an intermolecular effect not accounted for in existing theories is demonstrated by the unexpectedly large δT_c, 0.9 K, that was observed for the $Rb_3(^{13}C_{60})_{0.5}(^{12}C_{60})_{0.5}$ materials. These results are used to critically assess proposed mechanisms of fullerene superconductivity.

Metal-doped fullerenes represent a fascinating class of superconductors that can exhibit transition temperatures (T_c) in excess of 30 K (*1–5*). The existence of superconductivity at such surprisingly high temperatures has led to considerable speculation about the mechanism of superconductivity and about the possibility of achieving higher temperature transitions. Theoretical models put forth to explain the formation of Cooper pairs and superconductivity in the fullerenes range from conventional electron-phonon models (*6–9*) to purely electronic mechanisms (*10, 11*). An important assumption in both of these models is that superconducting pair formation is dominated by the properties of single clusters and that the bulk T_c can be obtained from a conventional mean-field average of the single cluster properties. Because the coherence length of the superconducting pairs is so short (≈25 Å) in the fullerene superconductors and because it is uncertain whether intercluster terms can indeed be ignored, it remains essential to probe the contributions of both the single cluster and the intercluster contributions to superconductivity.

Department of Chemistry and Division of Applied Sciences, Harvard University, Cambridge, MA 02138.

*To whom correspondence should be addressed.

We address here the open question of the mechanism of superconductivity in the fullerenes through systematic investigations of a series of ^{13}C-substituted Rb_3C_{60} superconductors for which the isotopic substitution within the solid is precisely controlled. The classic phonon-mediated pairing model of Bardeen, Cooper, and Schrieffer (BCS) (*12*) predicts that $T_c \propto M^{-\alpha}$, where M is the ionic mass and α is the isotope shift exponent. For simple metals, α equals 0.5. Electron-electron interactions in real materials may reduce the value of α below 0.5 (*13, 14*). Measurements of the isotope shift in Rb_3C_{60} have been made on materials containing poorly controlled isotopic distributions and $^{12}C_{60}$ impurity (*15–17*). Ramirez and co-workers (*15*) found that $\alpha \approx 0.37$ in samples containing, on average, 75% ^{13}C, whereas two other groups (*16, 17*) reported that α was >1 in samples containing smaller percentages of ^{13}C. In all of these studies the value of α was determined by extrapolating to 100% $^{13}C_{60}$ with little regard for the detailed composition of the starting material. The conflicting values for these extrapolated isotope shifts have made conclusions about the absolute magnitude of α and the mechanism of superconductivity unclear. To determine unambiguously the magnitude of α for Rb_3C_{60} and to elucidate the essential role of intercluster versus intramolecular in-